Surface barrier and lower critical field in $YBa_2Cu_3O_{7-\delta}$ superconductors

D.-X. Chen
Instituto de Magnetismo Aplicado, RENFE-UCM, 28230 Las Rozas, Madrid, Spain

R. B. Goldfarb and R. W. Cross
Electromagnetic Technology Division, National Institute of Standards and Technology, Boulder, Colorado 80303

A. Sanchez
Departament de Fisica, Universitat Autònoma de Barcelona, 08193 Bellaterra, Barcelona, Spain
(Received 5 February 1993)

The fields for first vortex entry and last vortex exit, H_1 and H_2, and the lower critical field H_{c1} for a grain-aligned, sintered $YBa_2Cu_3O_{7-\delta}$ superconductor have been determined from saturated magnetic-hysteresis loops using an extended critical-state model. For fields oriented along the grain c axis, H_1 increases with decreasing temperature, showing an upturn below 50 K, whereas H_2 remains small and positive, in general agreement with the theory of Bean-Livingston surface barriers. H_{c1} has a Bardeen-Cooper-Schrieffer temperature dependence above 50 K, but it rises at low temperatures. For fields oriented in the ab plane, H_{c1} has a similar temperature dependence, but surface barriers are not evident in the magnetization.

I. LOWER CRITICAL FIELD AND SURFACE BARRIERS

The lower critical field H_{c1} of high-critical-temperature (high-T_c) superconductors is an intrinsic parameter related to the mechanism for superconductivity. Measured values of the magnetic penetration depth $\lambda(T)$ generally follow the temperature dependence expected from Bardeen-Cooper-Schrieffer (BCS) theory.[1] This should lead to saturation in H_{c1} when $T < T_c/2$. For example, Wu and Sridhar[2,3] determined H_{c1} of $YBa_2Cu_3O_{7-\delta}$ (YBCO) monocrystals from rf measurements of $\lambda(T,H)$ and obtained a BCS-like temperature dependence. However, magnetic measurements of $H_{c1}(T)$ consistently show an upturn below $T_c/2$.[4–9] Such non-BCS behavior has been attributed to measurement error due to demagnetizing effects and volume flux pinning, which cause uncertainties in field values and round off the initial magnetization curve;[9,10] enhanced proximity-effect coupling between superconducting and normal atomic layers at low temperature;[11,12] and the presence of surface barriers, which increase the field for first vortex entry H_1 to above H_{c1}.[13–16]

If the surface-barrier effect becomes strong at low temperatures, an upturn in $H_1(T)$, which does not necessarily reflect the actual behavior of H_{c1}, may occur.[17] With this in mind, McElfresh *et al.*[8] incorporated a surface barrier in the critical-state model[18] for magnetization. They analyzed remanent magnetization M_r as a function of maximum applied field to see whether surface barriers affected the H_{c1} determinations. Their results did not show such an influence and, therefore, surface barriers were apparently unable to explain the upturn in H_{c1} at low temperatures. Burlachkov *et al.*[19] assumed the existence of a large surface barrier in an untwinned YBCO monocrystal at low temperatures. They postulated that flux penetration in such samples occurred through gates, where the barrier is suppressed by surface defects. They used locally semicylindrical penetrated-flux boundaries, rather than planar boundaries, and the Bean critical-state model. The magnetization deviation from linearity, δM, is usually proportional to $(H - H_{c1})^2$. However, with curved flux boundaries, δM was calculated to be proportional to $(H - H_{c1})^3$. An extrapolation gave low-temperature $H_{c1}(T)$ smaller than $H_1(T)$. These extrapolated values gave a smooth BCS-like curve when combined with direct high-temperature measurements of $H_1(T)$.

As summarized by Meilikhov and Shapiro,[20] the determination of $H_{c1}(T)$ in the presence of surface barriers remains to be explained. In this work, we study the effects of surface barriers and thermal-equilibrium magnetization M_{eq} on the saturated magnetization curves of polycrystalline YBCO, rather than on the initial curve or remanent magnetization. Compared to the large demagnetizing fields in platelike monocrystals, overall demagnetizing effects are minimized by small grains in a sufficiently long sintered sample, and the magnetic irreversibility due to volume pinning is much smaller. Fits to the hysteresis loops using an extended critical-state model[15,16] give values for the fields of first vortex entry and last vortex exit, H_1 and H_2, and the lower critical field H_{c1}. We conclude that, even if surface barriers and volume pinning are considered, there is a rise in H_{c1} at low temperatures. The rise may be intrinsically connected to the upturn in H_1 through the Bean-Livingston (BL) theory of surface barriers[21] and the phenomenological Ginzburg-Landau (GL) theory[22] for type-II superconductors; it could reflect an increase in the GL parameter κ at low temperatures.

In research on conventional superconductors, the sur-

face barrier was first explained by Bean and Livingston in terms of a surface-image force.[21] For increasing applied field H, for a perfect surface at 0 K, flux may not be able to enter until a field $H_1 \approx H_c/\sqrt{2}$, where H_c is the thermodynamic critical field. For decreasing H, the barrier to vortex exit does not disappear completely until $H = H_2 = 0$. The effect should be weakened by increasing temperature since vortices overcoming the barrier is a thermally activated process. After the first vortex entry, the barrier diminishes quickly with further increase of the applied field.[23] Experimental observation of the effect of the BL surface barrier in conventional type-II superconductors requires smooth sample surfaces.[24] In high-T_c superconductors, however, κ is on the order of 10^2. This causes H_c to be greater than H_{c1} by a factor of the same order. (Likewise, $H_c \gg H_1$.) Hence, the surface barrier may become prominent even for small grains without artificially prepared smooth surfaces.[13] For crystals with finite dimensions, demagnetizing effects and surface irregularities will reduce the barriers.[21]

II. EXPERIMENT AND DATA

A grain-aligned, sintered YBCO sample[25] was used for this study. Its dimensions were $3.1 \times 4.8 \times 4.8$ mm, with one long dimension parallel to the c axis and the other parallel to the ab planes of the grains. The sample density was 4.8 g/cm^3, and the grains were platelet shaped with average dimensions of 5 μm in the c axis and 20 μm in the a and b axes. Initial and descending magnetization curves for fields along the c axis and ab plane were measured at several temperatures after zero-field cooling. A commercial 5.5-T superconducting-quantum-interference-device-based magnetometer was used with a 4-cm scan length, corresponding to a field variation of 0.19%. The data were adjusted using a bulk demagnetizing factor of 0.24, deduced from low-field ac susceptibility measurements.

Several $M(H)$ curves for fields along the c axis measured at different temperatures are shown in Figs. 1(a) and 1(b). For each curve, besides a shoulder around $H = 0$ due to intergranular supercurrents, two common features can be visualized (if one completes the loop by adding a symmetric ascending curve): (1) The left and right portions of the loop are sheared vertically; (2) the maximum loop width ΔM is located on either side of zero field. (This behavior is general for sintered YBCO superconductors.) Compared with the usual critical-state loops, the former indicates nonzero H_{c1} and M_{eq}, whereas the latter reflects the effect of surface barriers.[15,16] These two extra contributions, together with the volume supercurrents, require the use of an extended critical-state model for describing magnetic properties.

III. EXTENDED CRITICAL-STATE MODEL FITS

The measured descending $M(H)$ curves were fitted with the extended critical-state model introduced in Ref. 16, in which the local field-dependent volume critical current density was assumed to be exponential, $J_c(H_i) = J_c(0)\exp(-|H_i|/H_0)$, where H_i is the local internal field and $J_c(0)$ and H_0 are temperature-dependent constants. The segments for $|H| > H_1$ and $|H| > H_2$ of the surface-barrier-modified thermal-equilibrium magnetization curve $M_s(H)$ were simplified to be also exponential. By adjusting a field constant H_4, strong (small H_4) or weak (large H_4) field dependence of M_s within the exponential segments can be obtained.

An example of the fitting results is given in Fig. 2(a) for the 50-K loop. The solid line is the low-field fitting curve from which H_1 and H_2 are determined; the dashed line is the high-field fitting curve from which H_{c1} is obtained. The $M_s(H)$ curve deduced from the low-field fit is shown in Fig. 2(b), where the three fields are identified.

A. Uniqueness of fits

The details of the fitting procedure are described in Ref. 16. The following approach makes the results

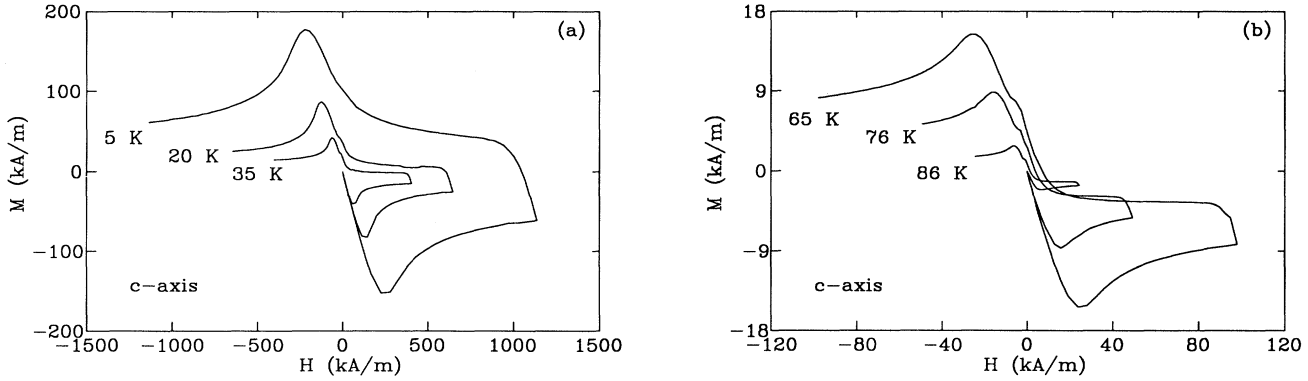

FIG. 1. Magnetization curves at several temperatures for grain-aligned, sintered $YBa_2Cu_3O_{7-\delta}$ for applied field along the c axis: (a) 5–35 K, (b) 65–86 K.

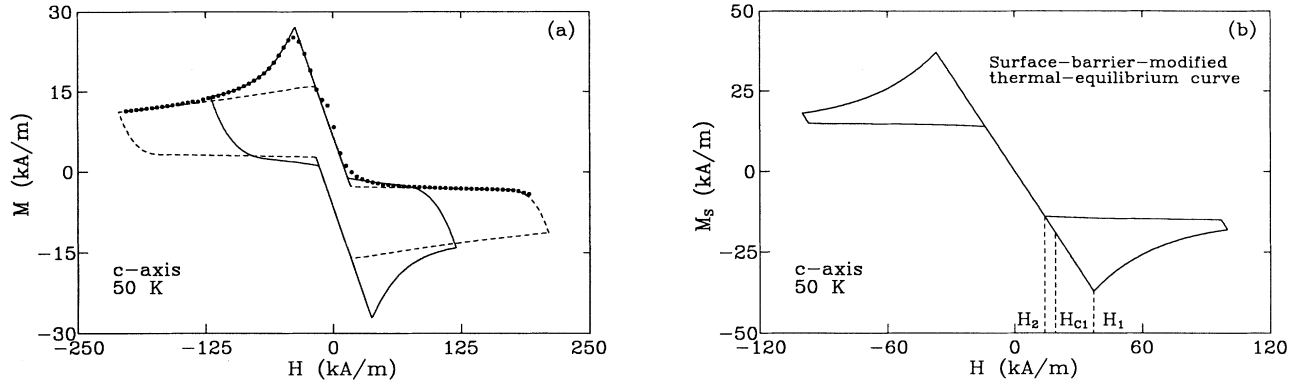

FIG. 2. (a) Extended critical-state model fitting curves to the magnetization loop at 50 K. Solid line: low-field fit to derive H_1 and H_2. Dashed line: high-field fit to derive H_{c1}. (b) $M_s(H)$ deduced from the low-field fit. H_1, H_2, and H_{c1} are noted.

unique: The high-field fit is performed first. Here, a null surface-barrier contribution is assumed because of the quickly diminished barriers at high fields. This condition is expressed as $H_{1h} = H_{2h} = H_{c1}/1.1$, where the subscripts h indicate that H_{1h} and H_{2h} are simply high-field fitting parameters, not related to the low-field surface barrier. The second equality is an estimate based on the curvature of the $M_{eq}(H)$ curve approaching H_{c1}; it is explained below. Furthermore, a large value of H_4 was used, which corresponds to an almost linear $M_{eq}(H)$ curve above H_{c1}, justified by a large κ. Under these conditions, not only H_{c1} but also $J_c(0)$ and H_0 are determined. The second, low-field fit uses these values of $J_c(0)$ and H_0; actual values of H_1 and H_2 are determined by fitting the two rounded corners on the descending magnetization curve with sharp corners that both deviate from the data by the same amount. We were unable to accurately apply this last rule to the 5-K and 12-K H_2 data; they were determined by extrapolation from the data at 20 and 35 K. Within these guidelines, the precision in H_2 ranges from 0.2 kA/m at high temperatures to 2 kA/m at low temperatures. The precision in H_1 and H_{c1} is always better.

B. $H_1(T)$, $H_2(T)$, and $H_{c1}(T)$ along the c axis

As functions of temperature, H_1 and H_2 determined by the low-field fits are shown in Fig. 3(a). With decreasing temperature, H_1 increases linearly, followed by an upturn below 50 K. H_1 is often mistaken for H_{c1}; the temperature dependence of H_1 in Fig. 3(a) is in good agreement with those for H_{c1} reported by others.[5,8] The temperature dependence of H_2 is different; it takes small positive values for all temperatures. The extended critical-state model predicts that if $H_2 \geq 0$, the remanent magnetization M_r will depend only on volume supercurrents; that is, there is no surface-barrier contribution to M_r. Thus, the failure to detect a surface-barrier effect on H_{c1} from the remanent magnetization[8] is understandable.

Since $M_{eq}(H)$ of type-II superconductors is not linear when $H > H_{c1}$, H_{1h} (and H_{2h}) obtained from the high-field fits must be less than H_{c1}. However, it should be close to H_{c1} if κ is large, since the departure from linearity is small. From the theoretical $M_{eq}(H)$ curves given in Ref. 19 we estimate and define $H_{c1} = 1.1H_{1h}$ for $\kappa \approx 100$ and our fitting interval. The H_{c1} thus calculated is plotted in Fig. 3(b) as a function of temperature.

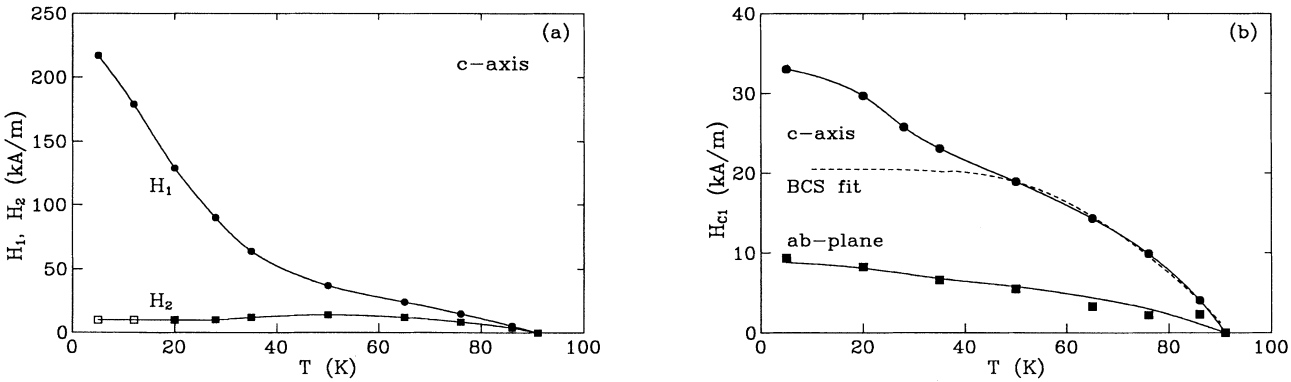

FIG. 3. (a) H_1 and H_2 along c axis determined by low-field extended critical-state model fits. (b) H_{c1} determined by high-field extended critical-state model fits (symbols). Dashed line is high-temperature BCS fit for c axis. Solid line for ab plane is calculated from H_{c1} data along c axis using Eq. (2).

C. Negligible surface barriers in the *ab* plane

The $M(H)$ curves measured along the *ab* plane are different, and there is no systematic evidence of surface barriers. This is unusual considering that it is the orientation for which a surface barrier would be most expected, with the field parallel to the largest grain surface. Moreover, a theoretical treatment based on anisotropic London theory concluded that the field of surface-barrier disappearance, that is, H_1, should be almost the same along the *c* axis and *ab* plane.[26,27] Our H_{c1} are obtained by high-field fits with an error of about 1 kA/m. They are plotted in Fig. 3(b) and have values smaller than H_{c1} along the *c* axis by a factor of about 3.5.

IV. COMPARISON WITH GINZBURG-LANDAU THEORY

Since H_{c1} along the *c* axis was determined with higher precision, we focus on its analysis. Our value of $H_{c1}(0\ \mathrm{K})$ is half as large as that determined by Wu and Sridhar.[2] Furthermore, our entire $H_{c1}(T)$ curve cannot be fitted by a simplified BCS clean-limit relation $H_{c1} \propto \lambda^{-2}$. A partial fit using the analysis given in Ref. 28 at high temperatures shown in Fig. 3(b) leads to an energy gap $2\Delta(0) = 3.6kT_c$, where k is Boltzmann's constant. Below 50 K, the data points are above the fitting curve.

To evaluate our H_{c1} results, we compare them with GL theory. The London-model formulas for anisotropic H_{c1} may be written as[29]

$$H_{c1,c} = \frac{\Phi_0}{4\pi\mu_0\lambda_{ab}^2}\left(\ln\frac{\kappa}{\sqrt{m_c}} + 0.50\right), \tag{1}$$

$$H_{c1,ab} = \frac{\Phi_0}{4\pi\mu_0\lambda_{ab}\lambda_c}\left(\ln\frac{\kappa}{\sqrt{m_{ab}}} + 0.50\right), \tag{2}$$

where λ is the penetration depth, κ is the GL parameter, and m is the anisotropic effective mass. The numerical evaluation of the constant 0.50 (for isotropic materials) is due to Hu.[30] For H_{c1}, subscripts *c* and *ab* denote the direction of the field; for λ and m, they denote the direction of the current. Since the properties along the *a* and *b* axes are similar, we use their geometric average, symbolized by *ab*. Typical values for YBCO superconductors, as summarized in Ref. 29, are $\lambda_{ab}(0\ \mathrm{K}) = 0.14\ \mu\mathrm{m}$, $\lambda_c/\lambda_{ab} = 5$, $m_{ab} = 0.34$, and $m_c = 8.8$. In the Lawrence-Doniach model for Josephson-coupled layered superconductors, applicable at low temperatures and for H parallel to the *ab* plane, the coherence length ξ_c, implicit in κ in Eq. (2), is replaced by the stacking periodicity.[31]

Substituting our value $H_{c1,c}(5\ \mathrm{K}) = 33$ kA/m in Eq. (1), we get $\kappa = 250$, in good agreement with the generally accepted value 10^2. In contrast, if we substitute the $H_{c1}(0\ \mathrm{K})$ values given by Wu and Sridhar[2] in Eqs. (1) and (2), we obtain contradictory and unphysical values of κ: $\sim 5 \times 10^4$ from Eq. (1) and $\sim 10^6$ from Eq. (2). Thus, although they demonstrated a consistency between λ and H_{c1} based on BCS theory, their results are inconsistent with Eqs. (1) and (2). Their use[3] of λ_{ab} with the isotropic GL formula for H_{c1} is not justified.

The BCS temperature dependence of H_{c1} implies temperature-independent κ, m_c, and m_{ab}. If the anisotropy is independent of temperature, we obtain, from $H_{c1}(0\ \mathrm{K}) = 20.5$ kA/m in our BCS fit, $\kappa = 38$ for $T > 50$ K. Therefore, the two-stage $H_{c1}(T)$ could be understood in terms of a temperature-dependent κ, which equals 38 above 50 K but increases to 250 as $T \to 0$. Calculation of $H_{c1,ab}(T)$ using the κ obtained from the $H_{c1,c}(T)$ data and Eq. (2) gives results consistent with the experimental data, as seen from Fig. 3(b). Thus, the anisotropic $H_{c1}(T)$ we obtain is consistent with anisotropic GL theory if a temperature-dependent κ is assumed. However, our value of $\kappa = 38$ is smaller than values deduced from high-temperature, high-field $M_{\mathrm{eq}}(H)$ measurements by ourselves and by others.[32] A large change in κ with temperature is not expected from BCS theory.[33]

We next examine our $H_1(T)$ curve. According to BL theory, H_1 should be proportional to H_c if thermal activation is negligible, as explained in Sec. I. This condition is satisfied for our sample, since there is no observable relaxation below H_1 on the initial curve. Therefore, the upturn in $H_1(T)$ should be a consequence of the same behavior in $H_c(T)$.

Equation (1) can be rewritten in terms of H_c as

$$H_{c1,c} = \frac{H_c\sqrt{m_c}}{\sqrt{2}\kappa}\left(\ln\frac{\kappa}{\sqrt{m_c}} + 0.50\right). \tag{3}$$

We see from Eq. (3) that H_c should be roughly proportional to κ at low temperatures since $H_{c1,c}$ and the factor in parentheses are almost constant. Therefore, a low-temperature increase in κ would imply a similar rise in H_c and H_1. However, the $H_c(T)$ values calculated from our $\kappa(T)$ and $H_{c1,c}(T)$ using Eq. (3) are too small to explain the observed BL surface barrier; $H_c(T)$ is only about 4 times the experimental $H_1(T)$ values instead of $H_c(T) \gg H_1(T)$. Thus, the magnetic behavior of YBCO is not perfectly consistent with GL theory. One could argue that κ is both temperature and field dependent, increasing with field between H_{c1} and actual H_c, but that is beyond the purpose of this paper.

V. CONCLUSION

In summary, we measured hysteresis loops of a grain-aligned YBCO sample along both the *c* axis and *ab* plane as functions of temperature. Demagnetizing effects were much smaller than those typically obtained in platelike monocrystals. The data were fitted with an extended critical-state model, which gives $H_{c1}(T)$ and the fields for first vortex entry and last vortex exit, $H_1(T)$ and $H_2(T)$. $H_1(T)$ along the *c* axis is in good agreement with values of fields identified by others as H_{c1} in monocrystals and is

qualitatively consistent with BL theory. Surface barriers in the *ab* plane were negligible.

Unlike some published results, our $H_{c1}(T)$ function does not follow BCS theory for $T < T_c/2$, even when surface barriers are considered. However, both $H_{c1,c}(T)$ and $H_{c1,ab}(T)$ agree well with GL theory as expressed by Eqs. (1) and (2) if κ is assumed to change from 38 above 50 K to 250 as $T \to 0$.

ACKNOWLEDGMENTS

The sample was provided by H. R. Hart, Jr. and A. R. Gaddipati, General Electric Company, Schenectady, NY. M. W. Coffey, T. M. Eiles, and A. Yu. Simonov offered critical comments and suggestions on the manuscript. This work was partially supported by a NATO Collaborative Research Grant.

[1] D. R. Hashman, L. F. Schneemeyer, J. V. Waszczak, G. Aeppli, R. J. Cava, B. Batlogg, L. W. Rupp, E. J. Ansaldo, and D. Ll. Williams, Phys. Rev. B **39**, 851 (1989).
[2] D.-H. Wu and S. Sridhar, Phys. Rev. Lett. **65**, 2074 (1990).
[3] S. Sridhar, D.-H. Wu, and W. Kennedy, Phys. Rev. Lett. **63**, 1873 (1989).
[4] J. P. Ströbel, A. Thomä, B. Hensel, H. Adrian, and G. Saemann-Ischenko, Physica C **153-155**, 1537 (1988).
[5] H. Adrian, W. Assmus, A. Höhr, J. Kowalewski, H. Spille, and F. Steglich, Physica C **162-164**, 329 (1989).
[6] A. Umezawa, G. W. Crabtree, K. G. Vandervoort, U. Welp, W. K. Kwok, and J. Z. Liu, Physica C **162-164**, 733 (1989).
[7] T. Ishii and T. Yamada, Physica C **159**, 483 (1989).
[8] M. W. McElfresh, Y. Yeshurun, A. P. Malozemoff, and F. Holtzberg, Physica A **168**, 308 (1990).
[9] L. Krusin-Elbaum, A. P. Malozemoff, Y. Yeshurun, D. C. Cronemeyer, and F. Holtzberg, Phys. Rev. B **39**, 2936 (1989).
[10] V. V. Moshchalkov, J. Y. Henry, C. Marin, J. Rossat-Mignod, and J. F. Jacquot, Physica C **175**, 407 (1991).
[11] T. Koyama, N. Takezawa, and M. Tachiki, Physica C **168**, 69 (1990).
[12] A. A. Golubov and V. M. Krasnov, Physica C **196**, 177 (1992).
[13] V. N. Kopylov, A. E. Koshelev, I. F. Schegolev, and T. G. Togonidze, Physica C **170**, 291 (1990).
[14] M. Konczykowski, L. I. Burlachkov, Y. Yeshurun, and F. Holtzberg, Phys. Rev. B **43**, 13707 (1991).
[15] D.-X. Chen and A. Sanchez, Phys. Rev. B **45**, 10793 (1992).
[16] D.-X. Chen, R. W. Cross, and A. Sanchez, Cryogenics **33**, 695 (1993).
[17] D. K. Finnemore, in *Phenomenology and Applications of High Temperature Superconductors,* edited by K. S. Bedell, M. Inui, D. E. Meltzer, J. R. Schrieffer, and S. Doniach (Addison-Wesley, Reading, MA, 1992), p. 164.
[18] C. P. Bean, Rev. Mod. Phys. **36**, 31 (1964).
[19] L. Burlachkov, Y. Yeshurun, M. Konczykowski, and F. Holtzberg, Phys. Rev. B **45**, 8193 (1992).
[20] E. Meilikhov and V. Shapiro, Supercond. Sci. Technol. **5**, S391 (1992).
[21] C. P. Bean and J. D. Livingston, Phys. Rev. Lett. **12**, 14 (1964).
[22] V. L. Ginzburg and L. D. Landau, Zh. Eksp. Teor. Fiz. **20**, 1064 (1950).
[23] J. R. Clem, in *Low Temperature Physics—LT 13,* edited by K. D. Timmerhaus, W. J. O'Sullivan, and E. F. Hammel (Plenum, New York, 1974), p. 102.
[24] J. D. Livingston and H. W. Schadler, in *Progress in Materials Science,* edited by B. Chalmers (Pergamon, Oxford, 1965), Vol. 12, p. 183.
[25] R. J. Loughran and R. B. Goldfarb, Physica C **181**, 138 (1991).
[26] V. P. Damjanović and A. Yu. Simonov, J. Phys. I (France) **1**, 1639 (1991).
[27] V. P. Dam'yanovich and A. Yu. Simonov, Sverkhprovodimost' **4**, 1512 (1991) [Superconductivity **4**, 1421 (1991)].
[28] M. Tinkham, *Introduction to Superconductivity* (McGraw-Hill, New York, 1975), pp. 34 and 63.
[29] J. R. Clem, Supercond. Sci. Technol. **5**, S33 (1992).
[30] C. R. Hu, Phys. Rev. B. **6**, 1756 (1972).
[31] J. R. Clem, M. W. Coffey, and Z. Hao, Phys. Rev. B **44**, 2732 (1991).
[32] Z. Hao, J. R. Clem, M. W. McElfresh, L. Civale, A. P. Malozemoff, and F. Holtzberg, Phys. Rev. B **43**, 2844 (1991).
[33] L. P. Gor'kov, Zh. Eksp. Teor. Fiz. **37**, 833 (1959) [Sov. Phys. JETP **37**, 593 (1960)].